This article has been accepted for publication in a future issue of this journal, but has not been fully edited. Content may change prior to final publication. Citation information: DOI10.1109/NANO51122.2021.9514342, Proceedings of the IEEE Conference on Nanotechnology

Biomass Combustion Fly Ash-Derived Nanoporous Zeolites for Post-Combustion Carbon Capture

Ben Petrovic, Mikhail Gorbounov, Abhishek Lahiri and Salman Masoudi Soltani

Department of Chemical Engineering, Brunel University London, Uxbridge UB8 3PH, United Kingdom

***Abstract*— Achieving negative CO_2 emissions via the combustion of sustainable biomass - known as bioenergy with carbon capture and storage - is inherently linked to the co-production of a significant amount of potentially hazardous waste combustion fly ash. Valorisation of this solid waste stream presents obvious economic, social, and environmental incentives within the context of waste utilisation and environmental protection. However, the origin of the biomass (the regional plantation) used during the combustion, dictates the physicochemical properties of this solid residue, making it suitable for specific applications while rendering it less favourable for others.**

In this study, a nanoporous zeolite as a CO_2 adsorbent has been synthesised from industrial-grade biomass combustion fly ash generated in one of the largest biomass combustion power plants in the UK. The method of nanoporous zeolite synthesis follows a fusion-assisted hydrothermal procedure and the produced nanoporous zeolite has been characterised by X-ray diffraction. The CO_2 adsorption investigations were conducted *via* thermogravimetric analysis to estimate the uptake capacity of the prepared adsorbents. TGA studies suggest that the nanoporous adsorbent, run under 100 mol% CO_2 at atmospheric pressure, has an equilibrium capacity of over 0.8 mmol$_{CO2}$/g at 50 °C. The characterisation results are in good agreement with our CO_2 adsorption data, demonstrating the nanoporous structure of our synthesised waste-derived zeolites.

I. Introduction

The climate crisis we are currently enduring is attributed to the emission of certain anthropogenic greenhouse gases which include carbon dioxide, methane and nitrous oxide. CO_2 however, has been, and still is considered the most significant of these gases especially when the extent of its emission is considered [1]. In 2019, the UK become the first major global economy to legislate for net-zero greenhouse gas (GHG) compared to 1990 levels by the year 2050 [2]. This climate emergency declaration was a result of sustained public pressure during the early summer. Since then, over 100 countries have followed suit and pledged for net-zero either on or before 2050 [3]. In the UK context, CO_2 emissions present over 80% of the GHG emissions during the years between 1990 and 2018 [4]. In order to successfully limit global temperature rise to less than 2 °C [5], technologies such as Carbon Capture and Storage (CCS) are indispensable. Post-combustion carbon capture (PCCC) refers to processes which involve the removal of CO_2 from various types of flue gases e.g. those generated at power plants, cement and steel manufacture. Whilst it may be possible to directly remove CO_2 from the atmosphere, the principal interests lie with the separation of CO_2 from large-point sources such as thermal power plants where the concentration of CO_2 is more favourable and the potential for emission reductions greatest [6].

In the Intergovernmental Panel on Climate Change's (IPCC) Fifth Assessment Report, 116 scenarios associated with an atmospheric concentration of CO_2 between 430 and 480 ppm in the year 2100 were identified, of which, 100 were dependent on the deployment of Bioenergy with Carbon Capture and Storage (BECCS) [7]. Although BECCS encompasses a group of technologies that span over a number of sectors, efforts have been focused on either BECCS *via* liquid biofuel production or BECCS *via* biomass conversion to heat and power. With the former predicted to account for over 60 % of the primary energy available for BECCS processes [8]. In the latter process, BECCS combines the combustion of sustainable biomass (a net-zero emission process) with PCCC. The conversion of biomass to heat through combustion, which assuming a mean ash yield of 6.8% [9] results in a significant quantity of co-generated waste fly ash. For example, during 2019, Drax power station burnt over 7 Mt of biomass enabling them to produce 12 % of the UK's renewable energy [10], this 13.4 TWh of energy accounts for around 40 % of the UK's total bioenergy production [11]. In the UK around 30 % of fly ash is directly landfilled [12] and given the concerns around environment contamination, dangerous alkalinity and leaching, valorisation of this waste is of paramount importance not just in the context of the environment, but also socially and economically [13]. Fly ash contains an abundance of raw aluminosilicates that can be converted into zeolites by well-documented procedures [14]. Zeolites are established solid sorbents for the selective adsorption of CO_2 in the post-combustion context [15], exploitation of this resource could be a simple yet efficiently viable route towards the accelerated deployment of BECCS in the UK and around the world.

II. Materials and Methodology

The biomass combustion fly ash (BFA) precursor employed in this work was collected from a biomass

This article has been accepted for publication in a future issue of this journal, but has not been fully edited. Content may change prior to final publication. Citation information: DOI10.1109/NANO51122.2021.9514342, Proceedings of the IEEE Conference on Nanotechnology

combustion facility in the UK. The BFA has been extensively characterised by Scanning Electron Microscopy (SEM, LEO 1455VP), Energy Dispersive X-Ray Spectroscopy (EDS, Edax International Ltd.), Fourier Transform Infrared spectrometry (FTIR, Perkin Elmer Spectrum One), X-Ray Diffraction (XRD, Bruker D8) and Particle Size Analysis (PSA, Beckman-Coulter LS230). The nanoporous zeolites were synthesized using a fusion-assisted, hydrothermal procedure [16], [17] to increase the solubility of the complex Si and Al species [14] in the BFA reducing the synthesis time whilst simultaneously increasing crystallinity and yield [14], [18] when compared to the conventional hydrothermal method [19].

The BFA (10g) was mixed with NaOH Pellets (16g, Sigma Aldrich) and ground in a pestle and mortar. This mixture was then fused in a muffle furnace at 550 °C for 1 hour after which the fusion product was cooled and ground in a pestle and mortar. Deionised water (100 ml) was then added to a PTFE liner followed by 13 g of the ground fusion product. This solution was then magnetically stirred at 300 rpm for 16 hours. Subsequently, the PTFE liner was inserted into a stainless-steel pressure digestion vessel (Berghof DAB-3) and then heated at 90 °C for 4 hours. The product was then separated *via* vacuum filtration, washed with deionized water until pH 7 and dried at 110 °C overnight. The produced zeolite has been characterized using XRD and evaluated for CO_2 adsorption performance *via* Thermal Gravimetric Analysis (TGA, TA Instruments Ltd. SDT-Q600). The adsorption performance the sample was measured at 50 °C, under a gas flow rate of 50 $mlmin^{-1}$ CO_2 (99.9%) at atmospheric pressure for 2 hours.

III. Results and Discussion

A. Biomass Fly Ash Characterization

Given the nature of BFA *i.e.* non-conductive, the sample was gold coated *via* the gold-sputtering technique and then used to assess its surface morphology. The SEM image can be seen in Fig. 1. The ash is comprised of a combination of spherical particles with wide size variation, agglomerations of these particles and a selection of porous elements. The spherical particles or cenospheres are typical of fly ash and can be attributed to their amorphous coating formed as a result of relatively abrupt cooling post-combustion [20]. It has also been observed that the cenospheres present hollow microspheres of aluminosilicate glass shells that possess inclusions of various crystalline phases such as quartz or mullite [16], [21].

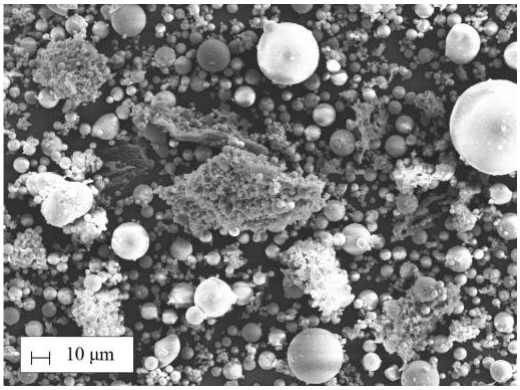

Fig. 1: SEM image of BFA, 15 kV, 300 pA and 1 kx mag.

The EDS analysis of this sample elucidated to the presence of a significant amount of oxygen, silicon, aluminium and calcium as well as potassium, iron, magnesium and sodium. Trace amounts of phosphorous and sulphur were also identified. The high prevalence of oxygen indicates that there exists a large quantity of oxides such as Al_2O_3 and SiO_2. Several areas were analysed, and an average weight percent of the elements present are exhibited in TABLE *1*.

TABLE 1*:* The EDS elemental analysis of the BFA.

Element	Weight (%)
Na	1.66
Mg	2.01
Al	9.15
Si	14.28
P	0.13
S	0.70
K	7.91
Ca	8.54
Fe	3.78
O	51.84

By mixing BFA with KBr powder and pressing into a disc, the infrared spectra collected in the region of 4000 – 450 cm^{-1} elucidated the presence of several bonds within the BFA. Most notably, the peaks at 1628.3 and 1384.85 cm^{-1} which were ascribed to the stretching and bending vibrations of the O-H bond [22], [23] present as either physisorbed moisture or hydroxides within the ash. The carbonyl group was identified at 1410.45 and 875.84 cm^{-1} and denoted as the asymmetric tensile stretching and bending vibrations of the double bond, respectively [24], [25]. Si-O bonds have also been identified at 1020.07 and 689.07 cm^{-1} typical of aluminosilicate structures [23], [26]. The substitution of Si atoms by Al in the tetrahedral position of the formation leads to a lower binding energy between the O and Si atoms which decreases the asymmetric stretching vibration band from c.1100 cm^{-1} for Si-O-Si compounds to a lower wave number for Si-O-(Al) bond types.

TABLE 2: Phases present in the XRD pattern and their associated powder diffraction files (PDF).

Phase	PDF
Lime	00-037-1497
Calcite	00-066-0867
Hematite	01-073-8431 00-024-0072
Portlandite	01-070-5492
Boehmite	00-021-1307
Potassium Oxide	01-077-2176
Kalicinite	01-070-0995
Periclase	01-071-1176
Mullite	01-074-4146
Quartz	01-074-1811

This article has been accepted for publication in a future issue of this journal, but has not been fully edited. Content may change prior to final publication. Citation information: DOI10.1109/NANO51122.2021.9514342, Proceedings of the IEEE Conference on Nanotechnology

The XRD pattern corroborated the EDS analysis although the presence of sodium and other trace elements was not observed. As expected, the fly ash is a mixture of aluminosilicates with an abundance of inorganic mineral phases such as metal oxides and carbonates.

TABLE *2* exhibits the phases that were identified during the analysis and the powder diffraction file (PDF) associated with each. Crystalline quartz, mullite, hematite, portlandite and calcite were registered which are all typical of fly ashes.

Particle size analysis of the BFA indicated 4 distinct peaks as can be seen in Fig. 2 which can be interpreted in two ways. The first being a distribution that possesses 4 distinct maximums at 12, 30, 70 and 161ums; the second being that the BFA is comprised of 2 independent bi-modal distributions of non-spherical particles, the aspect ratio of which can be inferred from the two peaks. However, since the BFA is seen to be predominately spherical, it can be assumed that the PSA identified a distribution with 4 distinct maximums.

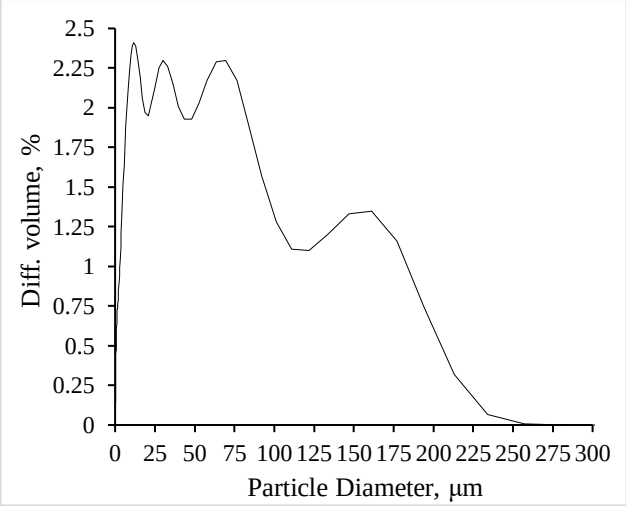

Fig. 2:Particle size distribution plot for raw-BFA.

B. Biomass Fly Ash Derived-Zeolite Characterisation

The diffractograms of the studied zeolite produced from BFA did not indicate pure crystalline phases. It is clear though, that no reflexes of the phases present in the raw BFA were found. This suggests that fusing the BFA with NaOH at 550 °C for 1 hour is suitable for the conversion of BFA into sodium silicate and sodium aluminate species which are favourable for the hydrothermal reaction [14]. However, the lack of distinct peaks representative of crystalline zeolites indicates that the conditions during the hydrothermal treatment may not be suitable for producing highly crystalline phases or that the scan duration in the XRD analyses is not sufficient.

C. CO_2 Adsorption Performance

The performance of the BFA-derived zeolite in the adsorption of CO_2 was evaluated using TGA apparatus. The adsorption kinetics curve can be seen in **Error! Reference source not found.** and demonstrates that the synthesised zeolite presents a CO_2 adsorption capacity of 0.825 $mmol_{CO2}/g$ at 50 °C. Additionally, it has been found that when regenerating the BFA-derived adsorbent, there is the potential for complete regeneration at 150 °C under nitrogen flow.

IV. Conclusion

This study suggests that the fusion-assisted hydrothermal method results in moderately zeolitic adsorbents that can effectively and reversibly adsorb CO_2. However, due to the inability to identify highly crystalline or pure zeolite phases within the product, manipulation of the experimental conditions during the hydrothermal treatment should result in more effective and better performing zeolitic adsorbents. The sorbent prepared in this work, showed a CO_2 update capacity of 0.825 $mmol_{CO2}/g$ at 50 °C under a pure CO_2 flow rate. Even with the lack of pure, crystalline zeolitic phases, the capacity demonstrated by the adsorbent is sufficient to suggest improvements can be made that would realise a competitive adsorbent for the removal or CO_2 from large-point sources. As a result, further investigations are deemed necessary to improve the adsorption capacity of this cost-effective waste-derived adsorbent, which may find great potentials in PCCC.

Acknowledgment

This work has been funded by the UK Carbon Capture and Storage Research Centre (EP/P026214/1) through the flexible funded research programme "Biomass Combustion Ash in Carbon Capture". The UKCCSRC is supported by the Engineering and Physical Sciences Research Council (EPSRC), UK, as part of the UKRI Energy Programme. The authors are grateful to the Research Centre for providing this funding. The authors would also like to acknowledge Brunel Research Initiative and Enterprise Fund (BRIEF) to support this work.

References

[1] A. Rafiee, K. Rajab Khalilpour, D. Milani, and M. Panahi, "Trends in CO2 conversion and utilization: A review from process systems perspective," *J. Environ. Chem. Eng.*, vol. 6, no. 5, pp. 5771–5794, 2018, doi: 10.1016/j.jece.2018.08.065.

[2] Committe on Climate Change and C. on C. Change, "Net Zero: The UK's contribution to stopping global warming," 2019.

[3] H. L. van Soest, M. G. J. den Elzen, and D. P. van Vuuren, "Net-zero emission targets for major emitting countries consistent with the Paris Agreement," *Nat. Commun.*, vol. 12, no. 1, Dec. 2021, doi: 10.1038/s41467-021-22294-x.

[4] P. Brown *et al.*, "UK Greenhouse Gas Inventory, 1990 to 2018. Annual Report for Submission under the Framework Convention on Climate Change," London, 2020.

[5] E. Commission and European Commission, "Paris Agreement | Climate Action," *European Commission Climate Action*, 2015. https://ec.europa.eu/clima/policies/international/negotiations/paris_en.

[6] E. I. Koytsoumpa, C. Bergins, and E. Kakaras, "The CO2 economy: Review of CO2 capture and reuse technologies," *J. Supercrit. Fluids*, vol. 132, no. July 2017, pp. 3–16, 2018, doi: 10.1016/j.supflu.2017.07.029.

[7] R. K. Pachauri *et al.*, *Climate change 2014: synthesis report. Contribution of Working Groups I, II and III to the fifth assessment report of the Intergovernmental Panel on Climate Change*. Geneva, Switzerland: Ipcc, 2014.

[8] M. Muratori, H. Kheshgi, B. Mignone, L. Clarke, H. McJeon, and J. Edmonds, "Carbon capture and storage across fuels and sectors in energy system transformation pathways," *Int. J. Greenh. Gas Control*, 2017, doi: 10.1016/j.ijggc.2016.11.026.

[9] S. V. Vassilev, D. Baxter, L. K. Andersen, and C. G. Vassileva, "An overview of the chemical composition of biomass," *Fuel*. 2010, doi: 10.1016/j.fuel.2009.10.022.

[10] Drax group, "Drax Annual Reports and Accounts," 2019.

[11] UK Committee on Climate Change, "Biomass in a low-carbon economy," 2018. https://www.theccc.org.uk/wp-content/uploads/2018/11/Biomass-in-a-low-carbon-economy-CCC-2018.pdf.

[12] U. Q. A. A. (UKQAA), "Ash Utilisation Data," 2018. http://www.ukqaa.org.uk/.

[13] J. Li, X. Zhuang, X. Querol, O. Font, and N. Moreno, "A review on the applications of coal combustion products in China," *Int. Geol. Rev.*, vol. 60, no. 5–6, pp. 671–716, 2018, doi: 10.1080/00206814.2017.1309997.

[14] C. Belviso, "State-of-the-art applications of fly ash from coal and biomass: A focus on zeolite synthesis processes and issues," *Prog. Energy Combust. Sci.*, vol. 65, pp. 109–135, 2018, doi: 10.1016/j.pecs.2017.10.004.

[15] B. Petrovic, M. Gorbounov, and S. Masoudi Soltani, "Influence of surface modification on selective CO2 adsorption: A technical review on mechanisms and methods," *Microporous Mesoporous Mater.*, no. October, p. 110751, Nov. 2020, doi: 10.1016/j.micromeso.2020.110751.

[16] S. Boycheva, D. Zgureva, H. Lazarova, and M. Popova, "Comparative studies of carbon capture onto coal fly ash zeolites Na-X and Na–Ca-X," *Chemosphere*, vol. 271, p. 129505, 2021, doi: 10.1016/j.chemosphere.2020.129505.

[17] D. Zgureva and S. Boycheva, "Experimental and model investigations of CO2 adsorption onto fly ash zeolite surface in dynamic conditions," *Sustain. Chem. Pharm.*, vol. 15, no. January, p. 100222, 2020, doi: 10.1016/j.scp.2020.100222.

[18] A. Dindi, D. V. Quang, L. F. Vega, E. Nashef, and M. R. M. Abu-Zahra, "Applications of fly ash for CO2 capture, utilization, and storage," *J. CO2 Util.*, vol. 29, no. November 2018, pp. 82–102, 2019, doi: 10.1016/j.jcou.2018.11.011.

[19] S. S. Bukhari, J. Behin, H. Kazemian, and S. Rohani, "A comparative study using direct hydrothermal and indirect fusion methods to produce zeolites from coal fly ash utilizing single-mode microwave energy," *J. Mater. Sci.*, vol. 49, no. 24, pp. 8261–8271, 2014, doi: 10.1007/s10853-014-8535-2.

[20] D. Mainganye, T. V. Ojumu, and L. Petrik, "Synthesis of zeolites Na-P1 from South African coal fly ash: Effect of impeller design and agitation," *Materials (Basel).*, 2013, doi: 10.3390/ma6052074.

[21] S. V. Vassilev, R. Menendez, M. Diaz-Somoano, and M. R. Martinez-Tarazona, "Phase-mineral and chemical composition of coal fly ashes as a basis for their multicomponent utilization. 2. Characterization of ceramic cenosphere and salt concentrates," *Fuel*, vol. 83, no. 4–5, pp. 585–603, Mar. 2004, doi: 10.1016/j.fuel.2003.10.003.

[22] M. Gómez *et al.*, "Development of mesoporous materials from biomass ash with future applications as adsorbent materials," *Microporous Mesoporous Mater.*, vol. 299, no. January, p. 110085, Jun. 2020, doi: 10.1016/j.micromeso.2020.110085.

[23] W. Mozgawa, M. Król, J. Dyczek, and J. Deja, "Investigation of the coal fly ashes using IR spectroscopy," *Spectrochim. Acta - Part A Mol. Biomol. Spectrosc.*, vol. 132, pp. 889–894, Nov. 2014, doi: 10.1016/j.saa.2014.05.052.

[24] M. Assad Munawar *et al.*, "Biomass ash characterization, fusion analysis and its application in catalytic decomposition of methane," *Fuel*, vol. 285, no. May 2020, p. 119107, Feb. 2021, doi: 10.1016/j.fuel.2020.119107.

[25] P. Chindaprasirt and U. Rattanasak, "Characterization of porous alkali-activated fly ash composite as a solid absorbent," *Int. J. Greenh. Gas Control*, vol. 85, no. March, pp. 30–35, 2019, doi: 10.1016/j.ijggc.2019.03.011.

[26] Y. Chen, C. Zou, M. Mastalerz, S. Hu, C. Gasaway, and X. Tao, "Applications of Micro-Fourier Transform Infrared Spectroscopy (FTIR) in the Geological Sciences-A Review," 2015, doi: 10.3390/ijms161226227.